Landscape-scale flow patterns over a vegetated tidal marsh and an unvegetated tidal flat : implications for the landform properties of the intertidal floodplain

Reference:

Vandenbruwaene Wouter, Schwarz Christian, Bouma T.J., Meire Patrick, Temmerman Stijn.- *Landscape-scale flow patterns over a vegetated tidal marsh and an unvegetated tidal flat : implications for the landform properties of the intertidal floodplain*

Geomorphology - ISSN 0169-555X - 231(2015), p. 40-52

DOI: http://dx.doi.org/doi:10.1016/j.geomorph.2014.11.020

Title page

Landscape-scale flow patterns over a vegetated tidal marsh and an unvegetated tidal flat: implications for the landform properties of the intertidal floodplain

W. Vandenbruwaene[1,2,*]; C. Schwarz[1]; T.J. Bouma[3]; P. Meire[1] and S. Temmerman[1]

[1]Ecosystem Management research group, Department of Biology, University of Antwerp, Universiteitsplein 1-c, B-2610 Wilrijk, Belgium

[2]Now at Flanders Hydraulics Research, Flemish Government, Berchemlei 115, B-2140 Antwerp, Belgium

[3]Royal Netherlands Institute for Sea Research (NIOZ; former NIOO-CEME), Yerseke, The Netherlands

*Corresponding author. Flanders Hydraulics Research, Flemish Government, Berchemlei 115, B-2140 Antwerp, Belgium, Tel. +32 3 224 61 81, E-mail wouter.vandenbruwaene@mow.vlaanderen.be

Abstract

Vegetation is increasingly recognized as an important control on flow and landform patterns in many landscape types. Field studies on the landscape-scale effect of vegetation in fluvial and tidal floodplains are relatively scarce while insights are especially based on flume and numerical models. Large-scale flow patterns and landforms were measured on a vegetated tidal marsh and unvegetated tidal flat, in particular dynamic changes in two-dimensional water surface slopes, flow velocities and directions on an extensive network of locations. It was found that during flooding and drainage of the vegetated tidal marsh, the flow was concentrated in and routed through bare tidal channels, whereas on the unvegetated tidal flat more homogeneous sheet flow occurred. On the marsh the peak flow velocities were lower on the vegetated platform (<0.1 m/s) compared to their adjacent tidal channels (0.3-1 m/s), while on the bare tidal flat the channel and platform flow velocities were not significantly different from each other (0.1-0.4 m/s). Further, the channel flow velocity pulse associated with the flooding and drainage of the adjacent platform differed between the marsh and mudflat system. This difference in the flow patterns has important implications for the landform differences between vegetated and bare tidal floodplains: (1) for tidal channels with channel widths smaller than 10 m, width-to-depth ratios (=β) were smaller for the tidal marsh channels (β~3) than for the tidal flat channels (β~9) (due to flow concentration towards the channels in the marsh); and (2) the vegetated marsh platform exhibits a clear levee-basin topography (due to vegetation-induced platform flooding from the channels), while there is no levee-basin topography on the bare flat (due to sheet flow). This study not only emphasizes previous findings on the direct effect of vegetation, acting as frictional constraints on flow in tidal marshes,it also suggests that the indirect effect of vegetation, namely its induced micro-topography, influences the flooding and drainage behavior of marsh systems potentially altering feedbacks caused by direct vegetation effects.

Keywords: intertidal landscape; tidal marsh and tidal flat; vegetation; flow patterns and landforms; tidal channels and intertidal platform

1. Introduction

It is increasingly recognized that landscape formation and evolution is governed by mutual interactions between biological and physical components of landscapes, so-called bio-geomorphic feedbacks (Corenblit et al., 2008; Murray et al., 2008; Reinhardt et al., 2010). For example, the establishment of vegetation in an initially bare landscape modifies the patterns of water and airflow and of sedimentation and erosion, while the modified flow patterns and landform evolution influence the spatial patterns of vegetation establishment and dieback. These biological-physical feedbacks may lead to landform patterns that are distinctively different between a vegetated or bare landscape state. This has been illustrated for several landscape types, such as intertidal floodplains (e.g., D'Alpaos et al., 2007; Kirwan and Murray, 2007; Temmerman et al., 2007), alluvial floodplains and channel patterns (e.g., Murray and Paola, 2003; Tal and Paola, 2007; Braudrick et al., 2009; Larsen and Harvey, 2011), dune landscapes (e.g., Baas and Nield, 2007), and hillslopes (e.g., Collins et al., 2004; Istanbulluoglu and Bras, 2005). While the above-cited studies are especially based on numerical simulation models or scaled flume experiments, field studies that systematically compared flow properties and landform patterns between a bare and vegetated landscape state are scarce (Dietrich and Perron, 2006; Temmerman et al., 2012).

For fluvial and tidal floodplains, recent flume experiments have demonstrated that the addition of vegetation patches significantly modifies the flow hydrodynamics and sedimentation-erosion patterns both inside and around the vegetation patches (Bouma et al., 2009; Rominger et al., 2010; Zong and Nepf, 2010; Vandenbruwaene et al., 2011). On the

77 larger landscape-scale, scaled flume experiments have shown that vegetation encroachment
78 on a fluvial floodplain leads to drastic changes in river channel patterns (Tal and Paola, 2007;
79 Braudrick et al., 2009). Hence these studies suggest that floodplain vegetation not only affects
80 flow patterns and landform evolution within the vegetated area itself, but also in the
81 unvegetated zones that occur adjacent to the vegetation.

82 Intertidal floodplains typically consist of a rather flat platform that is either of low-
83 elevation (within the tidal frame) and unvegetated (i.e., tidal flats) or of high-elevation and
84 vegetated (i.e., tidal marshes), and that is dissected by a branched network of bare tidal
85 channels. During the long-term (10–100 years) evolution of a tidal landscape, sediment
86 accretion may lead to an increase in tidal flat platform elevation and thus lower inundation
87 frequencies and durations, and hence vegetation may start to colonize the intertidal platform
88 (French and Stoddart, 1992). At this vegetated stage, a rapid increase in flow resistance over
89 the intertidal platform occurs. This increase is caused by: (1) the establishment of vegetation,
90 and (2) the decrease in inundation depth as the platform rises in the tidal frame (Nepf, 1999;
91 Allen, 2000; D'Alpaos et al., 2007;). Once the vegetated stage is reached, continued mineral
92 and organic sediment accretion direct the marsh platform towards a high equilibrium position
93 in the tidal frame (e.g., Pethick, 1981; Allen, 1990; Kirwan and Temmerman, 2009). There is
94 a special interest in the interactions between tidal marsh vegetation, tidal flow, and landform,
95 since these interactions are determinant for the ecosystem functions and services that tidal
96 marshes provide (Craft et al., 2008). Ecosystem services provided by tidal marshes range
97 from flood protection and shoreline erosion protection (through attenuation of waves and
98 storm surges), water quality improvement (through nutrient deposition and cycling),
99 biological productivity and coastal adaptation to accelerating sea-level rise (through sediment
100 accretion in balance with sea-level rise) (e.g., Craft et al., 2008, Kirwan et al., 2010, Mudd et
101 al., 2010; Temmerman et al., 2013). Further, the friction caused by tidal marsh vegetation is

also considered to be important for the attenuation of landward-propagating storm surges, and hence contributes to the protection of coastal communities against flooding (e.g., Wamsley et al., 2010; Temmerman et al., 2013).

Recent insights on the vegetation-flow-landform interactions in tidal marshes basically stem from numerical modeling studies, while empirical field studies that quantified the impact of intertidal vegetation on large landscape-scale flow patterns and landforms are scarce. Hydrodynamic modeling of tidal marshes has highlighted that tidal flow and sediment transport patterns are strongly affected by the presence or absence of marsh vegetation (Lawrence et al., 2004; Temmerman et al., 2005b; Blanton et al., 2010), while morphodynamic models have simulated the longer-term vegetation effects on landform evolution (Mudd et al., 2004; D'Alpaos et al., 2006; D'Alpaos et al., 2007; Kirwan and Murray, 2007; Marani et al., 2007; Temmerman et al., 2007; Mariotti and Fagherazzi, 2010). Hydrodynamic modeling showed that in these developing systems (i.e. where platform elevation is not yet in equilibrium with mean high water level, MHWL) vegetation-induced friction leads to strong reduction of flow velocities on the vegetated platform, combined with flow concentration and acceleration towards the bare channels that dissect the platform (Lawrence et al., 2004; Temmerman et al., 2005b). Consequently the rising water floods the vegetated platform from the channels and subsequent drainage of the platform is concentrated towards the channels (e.g. Christiansen et al. 2000; Temmerman et al. 2012). Hydrodynamic modeling and field studies further demonstrated that if all vegetation is removed from the platform, flow velocities through the channels and over the platform become similar, so that platform flooding and drainage occurs as a more homogeneous sheet flow that spills over the channels (Temmerman et al., 2005b, Temmerman et al., 2012). More longer-term morphodynamic simulations indicated that this vegetation effect causes the erosion of channels in intertidal landscapes (Temmerman et al., 2007) and effects the cross-sectional

dimensions of tidal channels (D'Alpaos et al., 2006). However, D'Alpaos et al. (2006) further demonstrated that in microtidal regimes the vegetation effect on channel erosion becomes overruled as the tidal marsh further increases in elevation within the tidal frame (towards a mature system, i.e. platform elevation is approaching MHWL), resulting in a reduction of channel flow velocity and tidal prism, and hence leading to infilling of the tidal channels.

Existing hydrodynamic field studies are mostly based on measurements at specific locations or transects in a tidal marsh, either on the platform within and above the vegetation canopy (e.g., Leonard and Croft, 2006; Neumeier and Amos, 2006; Lightbody and Nepf, 2006) or on locations in the channels (e.g., Bayliss-Smith et al., 1979). However, few studies have aimed to quantify the landscape-scale interactions between platform and channel flow. For example, comparison of total flood discharges through a channel with water volumes stored above the platform at high tide indicated that the water that flows onto the intertidal platform is only partly transported as concentrated flow through the channel, while more than 50% of the water may be transported as sheet flow (French and Stoddart, 1992; Temmerman et al., 2005a). However, to our knowledge no field studies have quantified the effect of vegetation presence or absence on the large, landscape-scale flow patterns, by systematically comparing the two-dimensional flow patterns over a bare tidal flat and vegetated tidal marsh.

The landforms of tidal marshes have been studied quite intensively, with a focus on either the geometric properties of the channels or the micro-topography of the platform. The geometric properties of tidal marsh channels, such as the width, depth and cross-sectional area of channels at different locations in the channel network, have been related to the surface area of the corresponding watersheds, and to the tidal prism (i.e., water volume stored above the watershed at high tide) (Fagherazzi et al., 1999; Rinaldo et al., 1999; Marani et al., 2003; D'Alpaos et al., 2010). The platform morphology of tidal marshes is generally known to exhibit a vegetation-induced micro-topography of natural levees along the channel banks, and

basins or depressions that are a few decimeters lower and located further away from the channels (e.g., Temmerman et al., 2005b). However surprisingly, there are no studies in the literature, to our knowledge, that have systematically compared the influence of channel-platform landform properties between vegetated marshes and unvegetated tidal flats, and their influence on the system's flooding and drainage behavior.

In this study we quantified the flow and landform patterns (on a landscape scale) of the intertidal platform and the tidal channels, for an unvegetated tidal flat and a vegetated tidal marsh. We hypothesize that for a tidal marsh, the presence of vegetation and the low inundation depths lead to high flow resistance over the intertidal platform, and consequently to flow concentration towards the tidal channels. For the tidal flat on the other hand, flow resistance over the platform is lower (no vegetation, higher inundation depths), and as a consequence flow concentration towards the tidal channels will be restricted and sheet flow will prevail. Moreover, it is assumed that the differences in flow patterns between a tidal flat and a tidal marsh will lead to different landform patterns, both for the intertidal platform as for the tidal channels. The flow patterns in a vegetated tidal marsh and an unvegetated tidal flat were quantified by measuring dynamic changes in two-dimensional water surface slopes, flow velocities and flow directions on an extensive network of measuring locations. The channel geometric properties and platform micro-topography of the vegetated tidal marsh and unvegetated tidal flat were then quantified. The differences in landform properties between both systems were finally related to the differences in flow patterns.

2. Study area

This study is performed on a vegetated tidal marsh (Saeftinghe) and unvegetated tidal flat (Paulina) within the Scheldt estuary (Belgium, SW Netherlands) (Fig. 1a). The estuary is characterized by a semi-diurnal- meso- to macrotidal regime, with a mean tidal range at the

mouth of 4.46 and 2.97 m during spring and neap tides, respectively. Further upstream, the mean tidal range increases, respectively, towards 5.93 and 4.49 m near Temse, and then progressively decreases to 2.24 and 1.84 m near Ghent (Claessens and Meyvis, 1994). Due to the salinity gradient along the estuary, the tidal marshes bordering the stream channel can be subdivided into salt, brackish and freshwater tidal marshes (Fig. 1b) (for more detailed information about the Scheldt estuary, see e.g. Meire et al., 2005).

The vegetated tidal marsh of Saeftinghe is located in the brackish part of the estuary and has an intertidal area of about 3000 ha (Fig. 1b). Saeftinghe is a typical mature tidal marsh, with a mean platform elevation above the local mean high water level, a platform micro-topography of levees and basins, and a branched network of bare channels. In this study we focus on a marsh area of 650 by 450 m in the northeastern part of Saeftinghe (Fig. 1b, 2a). There the mean marsh platform elevation is 2.9 m NAP (i.e. the Dutch reference datum), which is 0.17 m above MHWL (Fig. 2c), with a standard deviation of 0.19 m. This means that the marsh platform is only flooded by spring tides, which can be about up to 0.6 m higher than the mean platform elevation. The marsh vegetation is dominated by *Elymus athericus*, a species that forms a dense vegetation cover and that has a mean canopy height during summer of 0.43 m with a standard deviation of 0.1 m. At some sites *Aster tripolium* and *Scirpus maritimus* are observed, and for the highest elevations in the most eastern part *Phragmites australis* is present.

The unvegetated tidal flat of Paulina is located along the saltwater part of the Scheldt estuary (Fig. 1b). Between the embankment and the tidal flat, a small salt marsh borders the tidal flat area (Fig. 2b). The maximum width of the bare Paulina tidal flat (i.e. shortest distance from marsh edge to the low water line) is nearly 550 m, and the length of the considered study area is 900 m. The elevation of the tidal flat gently decreases towards the low water line, under a mean soft slope of 0.18 % for the largest part of the tidal flat, and a

slightly steeper slope (0.3 %) for the area closer to the low water line. The mean elevation of the tidal flat platform is 0.18 m NAP, which is 2.18 m below local MHWL (Fig. 2d), with a standard deviation of 0.3 m. This means that the tidal flat is inundated by every semi-diurnal tide, also during neap tides. Several channel networks can be distinguished in the tidal flat area, with their network locations largely located in the zone more close to the low water line (Fig. 2b). One network (most western) has a larger extent and is connected with the tidal marsh channel network.

3. Methods

3.1 Spatio-temporal changes in two-dimensional water surface

In the tidal marsh water levels were measured at 10 locations in the channel network and at 10 locations on the vegetated marsh platform, with a denser grid of locations in the southern part of the study site (locations 12-16, Fig. 2a). Water levels were measured by use of a diver (Schlumberger, type DIVER). This device contains a water pressure sensor that records the water surface level, an internal battery and data logger. The manufacturer guarantees a maximum error of ± 1 cm on the water level measurements. The measuring frequency was set at 2 minutes to record the tidal water level movement. At every location, the divers were attached to poles that were fixed deeply into the ground. The x and y coordinates (relative to the Dutch coordinate system) of the poles were determined by use of a DGPS (Thales z-max, accuracy 1-2 cm). However, the elevation differences (z coordinates; in m NAP) between the divers' pressure sensors were measured with a higher precision by use of a total station (Sokkia SET510k, accuracy 1-3 mm). Hence the water levels measured relative to the divers' pressure sensors were recalculated to absolute water levels in m NAP. We consider a maximum error on the water level differences between the pressure sensors of ± 1.5 cm (combined error on diver and total station measurements). Divers were attached to

227 the poles about 5 cm above the sediment bed surface. On the tidal flat water levels were
228 measured at 6 locations in the channel network and at 10 locations on the tidal flat platform
229 (Fig. 2b). Installation of the divers and determination of the diver elevations was performed in
230 the same manner as for the tidal marsh. Water levels were measured on the tidal marsh from
231 the 19th to the 25th of August 2009 (high spring tides), and on the tidal flat from 27th of August
232 until the 2nd of September 2009 (mean tides).

233 The instantaneous differences in water levels between the channel and platform
234 locations were calculated in order to compare the rate of flood and ebb propagation through
235 the channel network and over the platform. This was done by calculating for every time step
236 (every 2 min.) the mean and standard deviation of the channel water levels and of the platform
237 water levels. For the tidal marsh we made a distinction between the highest tides (0.43-0.58 m
238 above the mean marsh platform elevation at high water) and medium high tides (0-0.43 m
239 above the mean marsh platform elevation at high water). The highest tides completely overtop
240 the marsh platform and submerge the vegetation canopy on most locations, whereas the
241 medium high tides overtop most parts of the platform but do not submerge the vegetation
242 canopy. For the tidal flat all observed inundation events completely flooded the platform, and
243 therefore only one group of platform-overtopping tides was considered.

244 Secondly, spatio-temporal changes in water levels were analyzed by calculating two-
245 dimensional water surfaces in different time steps during the flood phase (starting from the
246 time that all divers became flooded), and during the ebb phase (ending at the time just before
247 the first diver felt dry). Two-dimensional water surface maps were calculated in ArcGIS 9.2
248 by use of the "Topo to Raster" spatial interpolation tool. "Topo to Raster" is an interpolation
249 method specifically designed for the creation of hydrologically correct digital elevation
250 models (Hutchinson, 1989). It is optimized to have the computational efficiency of local
251 interpolation methods, such as inverse distance weighted (IDW), without losing the surface

continuity of global interpolation methods, such as kriging and spline. For the tidal marsh data, it turned out to be hydrologically more correct to add "observation" points along the stream threads of the channel network. Water level values were then interpolated to these additional "observation" points based on linear interpolation of the measured channel water levels, following the stream threads of the channels. Water surfaces maps for the tidal marsh were calculated then using all points as input, i.e. measured channel and platform water levels, and interpolated channel water levels.

3.2 Flow velocities and flow directions

At 5 locations in the tidal marsh (3 in the channels, 2 on the platform) and at 6 locations in the tidal flat (2 in the channels, 4 on the platform) flow velocities and flow directions were measured (see, respectively, Figs. 2a and 2b for locations). Flow measurements were performed with two Nortek Aquadopp Current Profilers (ADCPs) and one high resolution Nortek Aquadopp Current Profiler (HR ADCP). The two ADCPs were equipped with an acoustic frequency of 2 MHz, and were set to measure vertical velocity profiles with an interval of 0.1 m and a maximum profiling range of 4 m. The HR ADCP was also equipped with an acoustic frequency of 2 MHz, but was set to a vertical profile resolution of 0.01 m, corresponding with a maximum profiling range of 1.28 m. The accuracy of the (HR) ADCP devices is guaranteed by the manufacturer as a maximum error of 1% on the measured value ± 0.5 cm/s. The flow velocities in the north-, east-, and z-directions were averaged over time periods of 2 minutes (to obtain the same time intervals as for the water level measurements). Flow measurements were performed during the same periods for which water levels were measured. In the tidal marsh, the flow was measured first at locations A and B (Fig. 2a) during 6 tides between the 19th and the 22nd of August. During the subsequent 6 tides from the 22nd until the 25th of August, the ADCPs were moved to locations C, D and E.

277 The HR ADCP was each time placed at a platform location (locations B and C). On the tidal
278 flat, first 6 tides were measured from the 27th until the 30th of August at locations A, B and C
279 (Fig. 2b). Then all flow devices were relocated to locations D, E and F, and the subsequent 5
280 tides were measured from the 30th of August until the 2nd of September. The HR ADCP was
281 each time placed at the location with the highest elevation, and thus the lowest inundation
282 heights (locations C and E, Fig. 2b).
283 Flow velocities were analyzed for the different locations, by plotting the maximum depth-
284 averaged flood flow velocity of our platform stations relative to the maximum depth-averaged
285 flood flow velocity of our channel stations at their respective tides. We compared this
286 relationship between 2 locations at the marsh (platform location B relative to channel location
287 A, platform location C relative to channel location D) and 2 locations at the tidal flat
288 (platform location A relative to channel location B, platform location D relative to channel
289 location F) (Fig. 2). Pairs in channel and platform locations were chosen according to spatial
290 proximity. Moreover, flow velocities were analyzed for the different locations by plotting the
291 maximum depth-averaged flood flow velocity against the water depth (above mean platform
292 elevation) at high tide for all observed tides. We compared this relationship between 4 groups
293 of locations: (1) the channel and (2) platform locations on the bare tidal flat, (3) the channel
294 and (4) platform locations on the vegetated marsh. For the tidal flat we excluded the flow
295 measurements at locations C and E because they are located far from the in-channel
296 measurements (locations B and F, Fig. 2b) and are relatively close to the vegetated marsh
297 edge.
298 The flow directions were analyzed together with the two-dimensional water surface
299 maps, showing the spatio-temporal changes in water surface slopes and associated flow
300 directions during a tidal inundation cycle (see section 3.1). The calculated flow directions are
301 depth-averaged flow directions, averaged over a time period of two minutes (i.e. the same

time interval as for the water level measurements). To assess the vertical variation in flow direction we calculated for each time-averaged profile the 5^{th} and 95^{th} percentile values, based on the bin values of the profile. For the tidal flats and tidal marshes of the Western Scheldt estuary there is no significant difference in flow velocity under calm and windy conditions (Callaghan et al., 2010). This implies that wind energy is not sufficiently strong to alter tidal currents (both flow velocity and flow direction), and hence the presented variation on the depth-averaged flow velocity (by the 5^{th} and 95^{th} percentile values) is caused by variations in tidal movement and not by wind forcing.

3.3 Channel width w, depth d and cross-sectional area Ω

3.3.1 Topographic survey

On the tidal flat and in the tidal marsh the channel morphology was measured by topographic surveying using a total station. For parts of the channel networks, stream thread points were measured about every 2-10 m along the stream thread, together with two accompanying channel edge points (on both sides one). Using this method, the entire range of channel widths was covered in the tidal flat. For the tidal marsh, the same was done for the channels with comparable channel widths, and for a few locations with larger channel widths. For each cross-section (one stream thread point, two edge points), the channel width and channel depth were determined as, respectively, the planimetric distance between the two edge points, and the difference in elevation between the mean elevation of the two edge points and the elevation of the stream thread point. Differences between tidal flat and tidal marsh channel morphology were evaluated by plotting the channel width against the channel depth.

At locations where in-channel flow velocities were measured, cross-sectional areas were calculated based on topographic surveying of the channel cross-sections (see section 3.2).

3.3.2 Building a network skeleton

In addition to topographic surveying, channel geometric properties (channel width, depth, cross-sectional area and watershed area (for watershed area see section 3.4)) were determined by building a network skeleton. A network skeleton is the pattern that connects all loci of the channel centerlines (Fagherazzi et al., 1999), and in this way the entire network can be evaluated. Every point along the skeleton was located at the half of the channel width. This was done by construction of Thiessen polygons (in ArcGIS 9.2), based on the line features of the channel edges. For the tidal marsh the channel edges were delineated based on aerial photographs using the edge of the vegetated platform and the unvegetated channels. For the tidal flat the channel edges were constructed by connecting the measured edge points (see section 3.3.1). As a next step, point features were made every meter along the skeleton. For each of these points we calculated values for the considered geometric parameters.

For the channel width, first a distance raster (Euclidean distance) was created using the channel edges as the target. At the skeleton data points, the raster values represent half the channel width, and by attributing and multiplying the raster values with a factor two, the channel width was found.

The channel depth at the skeleton data points was calculated based on the found relationship between the channel width and the channel depth, which is different for the tidal marsh and the tidal flat study area (see section 3.3.1 and Fig. 7).

Finally, the channel cross-sectional area at every skeleton point was calculated based on the half ellipse method (Vandenbruwaene et al., 2012), according to:

$$\Omega = \frac{wd\pi}{6} \quad (1)$$

with Ω = the cross-sectional area (m^2), w = the channel width (m), and d = the channel depth (m).

3.4 Watershed area and mean overmarsh tidal prism

In terrestrial river networks watershed areas are exclusively delineated by topographic gradients, however, on intertidal flats topographic gradients are small and the topography is comparatively deeply submerged, so that water flow is mainly determined by water surface slopes (Rinaldo et al., 1999). To determine watershed areas in the Saeftinghe tidal marsh and the Paulina tidal flat, the following theoretical assumptions were made: (1) water over a platform is assumed to flow perpendicular away from the nearest stream thread (during flood tide) or perpendicular towards the nearest stream thread (during ebb tide); (2) the contributing watershed area increases along channels with increasing distance from channel heads, measured along the channel network. The watershed areas were calculated using the hydrology tools in the ArcGIS 9.2 software (Spatial Analyst extension). This algorithm is designed for terrestrial networks and requires as input a Digital Elevation Model. Based on the above-described assumption (1), a raster file representing the shortest distance between every platform raster cell and the nearest stream thread was first created. For assumption (2), the distance from the mouth (measured along the network) was spatially represented by an allocation raster file. By summing both raster files, a virtual Digital Elevation Model (DEM) was made, incorporating our postulated assumptions, which was used as input for the hydrology algorithm. As output a flow accumulation raster file was created returning the watershed surface areas along the stream threads.

The cross-sectional dimensions of tidal channels (width, depth, cross-sectional area) have traditionally been related to the spring tidal prism, which is the water volume that is transported during spring tides to and from the intertidal platform and that is considered as the maximum water volume that is discharged through the channel cross-section (Myrick and Leopold, 1963; O'Brien, 1969; Jarrett, 1976; D'Alpaos et al., 2010). For tidal marsh channels,

overmarsh tides (i.e. which overtop the marsh platform level) are especially relevant because maximum channel flow velocities typically occur when the surrounding platform is flooded and drained (e.g. Bayliss-Smith et al., 1979; Pethick, 1980; French and Stoddart, 1992). Here we relate geometric channel properties to the mean over-platform tidal prism, which is the mean tidal prism of all high tides (over a period of one year) that overtop and thus flood the intertidal platform. For the Saeftinghe tidal marsh, we found that the mean over-platform high water level (MOHWL) is 3.25 m NAP which corresponds with a mean overmarsh water depth (MOWD) of 0.35 m (mean platform elevation is 2.9 m NAP). For the Paulina tidal flat, the platform is flooded at every high tide, and consequently the MOHWL is equal to the MHWL (i.e., 2.26 m NAP). With a mean platform elevation of 0.18 m NAP, the tidal flat MOWD is hence equal to 2.08 m. By multiplying the watershed areas with the MOWD, the mean over-platform tidal prisms for the tidal marsh and tidal flat were calculated along the corresponding channel networks. By plotting the mean over-platform tidal prisms against the channel widths, channel depths and channel cross-sectional areas, the differences in channel-forming mechanisms between the tidal marsh and the tidal flat were evaluated.

3.5 Platform morphology

The presence of a levee-basin micro-topography on the intertidal platforms was studied by quantification of differences in platform elevation (using the LiDAR based Digital Elevation Models, see Figs. 2a, 2b) with increasing distance from the channel edges. We compared the elevations close to the channel edges ($\leq$ 4 m from the edge) with the elevations further away from the channels (> 20 m from the edge), both for the vegetated marsh platform and bare tidal flat platform, and tested whether these elevation differences were significant or not (two-sample t-tests).

4. Results

4.1 Mean water level differences between channels and platform

We observe for the tidal marsh that during flood tides the mean water levels are most of the time higher in the channels than on the adjacent platform, while during ebb tides the opposite is observed (Fig. 3a). The instantaneous water level gradients between the channels and the marsh platform hereby decrease with increasing water depth above the platform. For the highest observed inundation events that entirely overtop the marsh platform and that submerge the vegetation canopy on most locations (Fig. 3a, circles), the mean water level in the channels is up to 13 cm higher than above the marsh platform during the first 15 minutes of inundation of the platform. This water surface difference starts to decrease when the water level rises above the mean platform elevation plus one standard deviation (Fig. 3a), and becomes negligible by the moment that the water level reaches the mean vegetation canopy height (Fig. 3a). During the rest of the flood phase, when water levels exceed the mean vegetation height, the mean water levels are not significantly different between the channels and platform. During the ebb phase, this difference remains also insignificant until the water level drops again below the mean vegetation canopy height. From then on the water level above the platform stays higher than the water level in the channels. With decreasing water level, the water level difference between platform and channels increases up to 30 cm at the moment that all except one platform diver fall dry (Fig. 3a). For medium high inundation events that just overtop the marsh platform surface at most locations but that do not overtop the vegetation canopy (diamonds, Fig. 3a), very similar patterns are observed as described above. The differences between the mean water level in the channel and on the platform remain for almost the whole of the flood and ebb phase, and disappear only very close to the moment of high tide. These medium high inundation events do not overtop the mean

vegetation canopy height and thus no phases of flood and ebb flow occur with negligible mean water level differences between the platform and channels (Fig. 3a).

As opposed to the tidal marsh, there is no significant difference on the unvegetated tidal flat between the mean water level in the channels and above the platform (cf. Fig. 3a, 3b). The lack of difference between channel and platform water levels is observed for the entire period of tidal flat inundation (i.e. flood and ebb phase).

4.2 Spatio-temporal changes in two-dimensional water surfaces and flow directions

Contour maps of instantaneous water surfaces are shown for the highest observed tide in the tidal marsh (see also Fig. 3a, circles), for different time steps during the flood and ebb phase (Fig. 4a-d, time steps indicated on Fig. 3a by arrows a-d). During the flood phase at the time that all divers in the study area become flooded (arrow a, Fig. 3a), we observe that for the more downstream locations in the channel network (i.e. towards the mainstream channel of the estuary), the water level is higher than the water levels at the more upstream locations in the channel network (i.e., towards the channel heads) (Fig. 4a). Within the wide main channel (between most northern part of channel and location 18 in Fig. 4a) the average water surface slope is 0.0069 %, while in the smaller tributary channels there is a steeper water surface slope of 0.023 % (between location 10 and 11) and 0.096 % (between location 9 and 15). In contrast to these rather gentle water surface slopes within the channel network, the water surface slopes between the channels and adjacent platform locations are considerably steeper, e.g. up to 0.27 % between location 10 and 14. Water levels during the flood phase are thus higher in the channels as on adjacent platform locations (see also Fig. 3a). As the flood tide continues and most of the vegetation gets overtopped (arrow b, Fig. 3a), more large-scale sheet flow develops, which is directed from the mouth of the main channel towards the rest of the marsh area (Fig. 4b). During the ebb phase, similar flow patterns are observed in the

opposite direction. As long as the vegetation remains overtopped (arrow c, Fig. 3a), large-scale sheet flow occurs from the inner marsh towards the mouth of the main channel (cf. Fig. 4c). Later during the ebb, as soon as the top of the vegetation is getting emergent again (arrow d, Fig. 3a), the water levels are higher above the marsh platform than in the adjacent channels (Fig. 3a)

The flow directions that were recorded at the ADCP locations (Fig. 4) have a NE to SE orientation during the flood phase, and a NW tot NE orientation during the ebb phase (Fig. 4). However, for time steps close to high water level (Fig. 4b, 4c) some of the flow vectors have an orientation in a more or less opposite direction. During the flood phase, this is observed for the location closest to the mainstream channel of the estuary (location C, Fig. 4b), and for the ebb phase for the location furthest away from the mainstream channel (location E, Fig. 4c). The flow vectors in the channels (locations A, D and E) have an orientation which is parallel to the nearest channel edge, and in general the water levels are lower in the flow direction and higher in the opposite direction of the flow (cf. contour lines and flow vectors of locations A, D and E, Fig. 4). On the marsh platform (locations B and C), flow vectors also point to locations with lower water levels, expect for the first time step of the flood phase where this observation is less clear (cf. contour lines and flow vectors of locations B and C).

For the highest observed tide over the tidal flat, instantaneous water surface slopes are always less than 0.15 %, and we do not observe any differences in water level which are related to the tidal channel network (see Figs. 3b, 5). Based on the ADCP measurements we observe that during flooding the water flows from the tidal flat edge towards the marsh edge in a more or less southern direction (locations A-F, Fig. 5a). During the ebb phase the flow directions are towards the mouth of the estuary (northwestern direction) or towards the tidal flat edge (northern direction) (Fig. 5b).

476

477 **4.3 Flow velocities**

478 On the tidal marsh there is a large difference between the observed flow velocity in the
479 channel network and on the vegetated marsh platform (Fig. 6a). In the marsh channels at both
480 our measurement locations (AB and DC), the flow velocities were more than 10 times higher
481 than at the adjacent platform, while on the tidal flat similar flow velocities between channels
482 and adjacent platform were observed at all measurement locations (AB and DF). In tidal
483 marsh channels, maximum flood flow velocities range from 0.3 m s^{-1} up to 1 m s^{-1}, while on
484 the marsh platform all observed flow velocity maxima are below 0.07 m s^{-1} (Fig. 6b). The
485 mean flood flow velocity in the channels (0.61 m s^{-1}, Fig.6b black solid circle) is significantly
486 higher than the mean flood flow velocity on the vegetated marsh platform (0.03 m s^{-1}, black
487 solid triangle) (two sample t-test, $p<0.0001$). For the tidal flat, observed flow velocity maxima
488 range from 0.1 to 0.4 m s^{-1}. There is no significant difference between the mean maximum
489 flood flow velocity in the channels (0.26 m s^{-1}, Fig.6b black empty circle) and on the platform
490 of the tidal flat (0.19 m s^{-1}, Fig. 6b black empty triangle) (two sample t-test, $p=0.06$).

491

492 **4.4 Channel width versus channel depth**

493 As the channel width increases, the difference in channel depth between the tidal
494 marsh and the tidal flat channels decreases (Fig. 7). For the tidal flat the relationship between
495 the channel width and the channel depth is close to the 1:10 line, which means that with
496 increasing channel width the width-to-depth ratio (=β) remains more or less constant (mean
497 value of 8.6) (Fig. 7). For the tidal marsh the slope of the trend line is considerably lower than
498 the slope of the 1:10 line, which means that with increasing channel width the width-to-depth
499 ratio increases. The mean β value for the same range of channel widths on the marsh as

observed on the tidal flat is 2.7, however for the widest marsh channels β, already attains a value of 34.

4.5 Channel width, depth and cross-sectional area versus tidal prism

The channel width, depth and cross-sectional area generally increase with increasing tidal prism (Fig. 8a-8c). A comparison of the relationships between the tidal marsh and the tidal flat shows that for equal tidal prisms, the channel dimensions (depth, width and cross-sectional area) are larger for the tidal marsh than for the tidal flat. The strength of the increase in channel width with tidal prism is not constant over the entire range in channel width: for the larger tidal prisms, the increase in channel width is larger than for the smaller tidal prism and is even zero for the smallest tidal flat channels (Fig. 8a). Similar relationships are observed for the channel depth and cross-sectional area (increase in d and Ω with increasing tidal prism) (Figs. 8b, 8c), although the observed gradient in increase of channel property differ between the different geometric properties (w, d and Ω) (Figs. 8a-8c).

4.6 Platform morphology

The tidal marsh platform is characterized by a typical levee-basin micro-topography. Close to the channel edges (≤ 4 m) the levees have a median elevation that is 15 cm higher than the median basin elevation further away from the channel edges (> 20 m) (two sample t-test, $p<0.0001$) (Fig. 9). On the tidal flat, the platform close to the channel edges (≤ 4 m) has a median elevation that is 14 cm lower than further away from the channels (> 20 m) (two sample t-test, $p<0.0001$) (Fig. 9). Hence, a levee-basin microtopography is clearly absent on the tidal flat platform.

5. Discussion

Modeling studies have highlighted the role of vegetation for determining flow patterns and landform evolution of intertidal floodplains (e.g., Lawrence et al., 2004; Temmerman et al., 2005b, 2007; D'Alpaos et al., 2007; Kirwan and Murray, 2007) and fluvial floodplains (e.g. Murray and Paola, 2003; Tal and Paola, 2007; Larsen and Harvey, 2011). Nevertheless few field studies have systematically described and compared the large landscape-scale flow patterns and landform properties of a vegetated and bare floodplain. Here it has been shown that for a vegetated tidal marsh high in the tidal frame, flow velocities are strongly reduced on the vegetated platform, compared to flow velocities in bare tidal channels that dissect the vegetated platform (Fig. 6a). This can be explained by the high flow resistance on the marsh platform due to the presence of vegetation, its exerted friction and the low inundation depths, which leads to flow acceleration towards the channels. Although the lower tidal flat may be subjected to higher absolute flow velocities at mid-tide than the upper tidal marsh, which is subjected to slower flow velocities closer to the turning of the tide, our study is in accordance with previous studies that showed that, by removing vegetation at high elevated marsh platforms, over-marsh flow patterns are mainly caused by vegetation friction (Temmerman et al., 2012). As a consequence, the rising flood propagates faster through the bare channels than over the vegetated platform, and hence the platform is flooded from the channels (Figs. 3a, 4). During drainage, similar flow patterns occur but in opposite direction. These observed flooding and drainage directions are in agreement with previous findings in field studies (e.g., Christiansen et al. 2000; Temmerman et al., 2012). In contrast to a vegetated tidal marsh, on a unvegetated tidal flat low in the tidal frame, flow velocities did not exhibit differences between the channels and the platform (Fig. 6a). This lack of relative difference between channel and platform flow velocities is explained as the friction differences between the channels and the bare platform are rather small (no vegetation and higher inundation depths).

549 As a consequence, more homogeneous sheet flow occurs, with flood propagation that is as
550 fast through the channels as over the platform (Figs. 3b, 5).

551 The differences in flow hydrodynamics between a tidal marsh and a tidal flat imply
552 that sediment transport patterns and resulting landforms (tidal channels and platform
553 characteristics) are different between vegetated marshes and bare tidal flats. This underlines
554 previous findings stressing the role of vegetation friction in altering flow patterns
555 (Christiansen et al., 2000; Davidson-Arnott et al., 2002; Temmerman et al. 2012; Bouma et
556 al., 2013). For comparable channel widths, we observe for tidal marsh channels smaller
557 width-to-depth ratios (β~3) and thus larger channel depths than for tidal flat channels (β~9)
558 (Fig. 7). A smaller width-to-depth ratio for tidal marsh channels is also observed in other tidal
559 systems like the Venice lagoon (Marani et al., 2002). We argue that the high flow resistance
560 on the vegetated tidal marsh leads to higher bottom shear stresses in the channels due to flow
561 concentration (Fig. 6a), which consequently leads to larger channel depths. For the
562 unvegetated tidal flat, we observe no significant difference in flow velocity on the platform
563 and in the channels, and thus no flow concentration occurs. Vegetation not only has an effect
564 on the flow hydrodynamics above a tidal marsh, it also has an important effect in stabilizing
565 the marsh surface and strongly affects bank failure mechanisms (Garofalo et al., 1980; Marani
566 et al., 2003). However, since our two investigated systems also exhibit major differences in
567 tidal prism (Fig.2c, d) we cannot distinguish to what degree the observed larger channel
568 depths depend on differences in friction (vegetation) or tidal prism.

569 Plotting the channel width against the channel depths shows some important
570 differences between tidal marsh and tidal flat channels. However, to make a proper
571 comparison between the channels of the intertidal floodplain, channel dimensions should be
572 related to the actual volumes of water that are flowing through the channels. Relating channel
573 dimensions to the tidal prism or watershed areas has been demonstrated to be a good proxy

574 for comparing tidal marsh networks where the marsh platform elevation has a high position in
575 the tidal frame (e.g., Rinaldo et al., 1999). However, when comparing these relationships for a
576 high elevated tidal marsh and a low elevated tidal flat, it is observed that the channel
577 dimensions in a tidal marsh are several times larger (factor 5-200) than in a tidal flat (Figs. 8a-
578 8c). Based on the observed empirical relationships for tidal inlets, we would expect
579 comparable channel cross-sectional areas for comparable tidal prisms (e.g. O'Brien, 1931,
580 1969; Myrick and Leopold, 1963; Jarrett, 1976). These strong differences in tidal prism
581 versus channel dimension between both systems can potentially be explained by the observed
582 vegetation-induced flow patterns. For the tidal marsh, the flow is concentrated towards the
583 tidal channels as long as the vegetation is not overtopped (Figs. 4a, 4d). Once the vegetation
584 becomes overtopped, more large-scale flow patterns will prevail and sheet flow is dominant
585 (Figs. 4b, 4c). Previous field studies already suggested this concept of flow partitioning
586 (French and Stoddart, 1992; Temmerman et al., 2005a; Vandenbruwaene et al., 2013). In the
587 case of a tidal marsh with a *high* position in the tidal frame, and consequently with a mean
588 over-platform high water level (see section 3.4) within the vegetation canopy, the flow at
589 overmarsh tides is mainly concentrated towards the tidal channels and the calculated tidal
590 prism can be considered as a good proxy for the volume of water that is transported through
591 the tidal channels. However, for the tidal flat it is observed that sheet flow is dominant during
592 the entire tidal cycle (see Figs. 3b, 5a, 5b), and hence the calculated tidal prism is a very large
593 overestimation of the volume of water that is actually transported through the tidal channel
594 network. A second reason which may explain the differences in the relationships between the
595 tidal prism and the channel properties of the tidal marsh and the tidal flat (Figs. 8a-8c) is that
596 for both systems the same methodology is applied to calculate watersheds. Indeed, we observe
597 in a tidal marsh that water flows away (Fig. 4a) or towards (Fig. 4d) the nearest stream thread
598 when the water is within the vegetation canopy. This is according to the assumptions we made

599 to calculate watershed areas (see section 3.4). Moreover, these findings support previous
600 modeling work where watershed areas are determined based on the planar channel geometry
601 and the unchanneled flow lengths (Rinaldo et al., 1999; Marani et al., 2003). However, for the
602 tidal flat, such flow patterns are absent (Figs. 3b, 5), and hence the found watershed areas
603 calculated according to our assumptions (see section 3.4) might be an overestimation of the
604 actual watershed areas and thus the actual water volumes flowing through the channels.

605 The landform properties of a tidal marsh and a tidal flat not only differ with regard to
606 the tidal channels, but also with regard to the platform morphology. The vegetated marsh
607 platform is typified by the presence of a levee-basin topography (Fig. 2b, 9), which can be
608 attributed to the observation that the flow is routed through the channels and subsequently
609 flows from the channels over the platform, as stated by previous studies (Temmerman et al.,
610 2005b; 2012; Schwarz et al., 2014). The levee-basin topography is a result of vegetation
611 friction, and its resulting sediment transport patterns, which form the geomorphology of the
612 developed salt marsh. According to the observed flooding and drainage behavior on the tidal
613 marsh (Fig.4, 6b), it is suggested that the levee-basin topography can be regarded as an
614 indirect effect of vegetation, potentially further supporting the direct friction effect in altering
615 flow patterns. The observed effect that downstream marsh channel water levels are higher
616 than the water levels at more upstream network locations might be caused by damping of the
617 tidal wave while propagating through the channels. However this effect does not affect our
618 results since we focus on a relative comparison of platform flooding behavior. On the bare
619 tidal flat such a levee-basin topography is absent (Fig. 9) because sheet flow prevails there
620 instead of concentrated channel flow.

621 Our empirical findings support hydrodynamic modeling that showed similar effects of
622 the friction caused by vegetation on flow patterns over a tidal marsh (Lawrence et al. 2004;
623 Temmerman et al., 2005b). These simulations also showed that vegetation reduces the flow

velocities on the vegetated platform, combined with flow acceleration towards the bare channels. As a consequence the simulated flood propagation is faster through the bare channels, and the vegetated platform is flooded from the channels. When removing the vegetation-induced friction in the model, higher flow velocities were simulated above the platform combined with lower velocities in the channel, leading to more homogeneous flood propagation (Temmerman et al., 2005b). More or less similarly, recent flume experiments have demonstrated that addition of vegetation patches (in the order of a few m^2 large) reduces flow velocities within the vegetation patches, and at the same time accelerates the flow in the bare zones adjacent to the vegetation (Bouma et al., 2009; Rominger et al., 2010; Zong and Nepf, 2010; Vandenbruwaene et al., 2011). Our field data show that this vegetation effect in combination with a high position in the tidal frame (both leading to high flow resistance over the platform) is also responsible for the landscape-scale differences in flow patterns (i.e. indirect vegetation effect) between a vegetated and unvegetated tidal floodplain.

Our observations on the landform differences between a vegetated and bare tidal floodplain are also in agreement with morphodynamic modeling, showing that establishment of vegetation patches on an initially bare tidal flat causes flow concentration and channel erosion in between the laterally expanding vegetation patches; the same was observed from time series of aerial photos (Temmerman et al., 2007; Schwarz et al., 2014). Similarly, D'Alpaos et al. (2006) simulated the deeper erosion of a tidal channel as a consequence of vegetation establishment on the surrounding platform, and the associated flow acceleration towards the channel. It should be pointed out that, in contrast to this study, the elevation of the intertidal platform in D'Alpaos et al. (2006) was similar for the vegetated state as for the unvegetated state. In this study we observed that tidal marsh channels (surrounded by a platform with a high elevation in the tidal frame) have smaller width-to-depth ratios ($\beta \sim 3$), and thus larger channel depths, than tidal flat channels ($\beta \sim 9$) (dissected in a platform with a

649 low elevation in the tidal frame). This observation is valid for channel widths smaller than 10
650 m (Fig. 7).

651 As opposed to models, where vegetation can be added or removed, the differences we
652 observed in this study between a bare and vegetated tidal floodplain may be not exclusively
653 caused by the presence or absence of vegetation, since also other environmental variables
654 differ between a tidal flat and a tidal marsh. Because of the lower position in the tidal frame,
655 tidal flats are generally flooded by deeper water and for longer than tidal marshes (Fig. 3), and
656 hence the water volumes that flood to and drain from the platform during a tidal cycle (i.e.,
657 called the tidal prism) are larger than on a tidal marsh. Assuming the whole tidal prism be
658 transported through the channels, this would lead for a same watershed area to wider and
659 deeper channels in a tidal flat, but this is obviously not the case (Fig. 8). On the contrary, for
660 similar tidal prisms, the channel dimensions (depth, width and cross-sectional area) on the
661 tidal flat are smaller than on the tidal marsh (Fig. 8). This is in accordance with our flow
662 velocity observations (Fig. 6) that concentrated channel flow prevails on the tidal marsh
663 (which suggests that a larger portion of the tidal prism is transported through the channels in
664 the tidal marsh and hence leads there to larger channel dimensions), while on the tidal flat
665 sheet flow prevails (which suggests that a smaller portion of the tidal prism is transported
666 through the channels on the tidal flat and hence leads there to smaller channel dimension).
667 Another important difference between the studied tidal marsh and tidal flat is the micro-
668 topography of the platform. On the tidal marsh the levee-basin topography is distinctively
669 present (Fig. 9). The highest differences in channel water level and platform water level (up to
670 13 cm; Fig. 3) are observed as long as not more than 25 % of the levees are overtopped by the
671 water. Once more than 75% of the levees become flooded, the water level differences
672 decrease, and ultimately disappear by the time that all of the levee locations are submerged.
673 At the time of submergence of the levees, also the top of vegetation in the lower lying

depressions is submerged (Fig. 3a). Hence, we suggest that both vegetation friction (directly) as well as vegetation induced micro-topography of levees (indirectly) causes confinement of the flow and hence flow concentration towards the channels.

Apart from the specific case of intertidal floodplains, the results of this study have also implications for the vegetation effects that may be expected in fluvial (alluvial) floodplains and fans. In a series of scaled flume experiments, Tal and Paola (2007) showed that vegetation encroachment on an initially bare fluvial floodplain was associated with a change from a multiple braiding channel pattern to a single channel. The width-to-depth ratio, β, of the channels substantially decreased from the bare state (β~30) to the vegetated state (β~5) (Tal and Paola, 2010). In accordance with this, we found that the width-to-depth ratio of channels in the bare tidal flat were higher (β~9) than in the vegetated marsh (β~3) for comparable channel widths (Fig. 8). In both the fluvial and tidal case, this can be attributed to the effect of the floodplain vegetation on flow concentration towards the channels and hence deepening of the channels. This process was demonstrated in an experimental fluvial floodplain, where addition of vegetation on a point bar lead to flow reduction within the vegetation and flow acceleration and increased erosion next to the vegetation (Rominger et al., 2010). The effect of tidal floodplain vegetation on the formation of a levee-basin topography may be also expected in fluvial floodplains, although we did not find studies that systematically compared the presence or absence of levee-basin topography on vegetated and bare fluvial floodplains.

6. Conclusions

In this research the flow hydrodynamics of the intertidal landscape for the two different landscape states were studied: (1) a landscape state with a high resistance against flow (tidal marsh) caused by the presence of a vegetated platform with a high position in the

tidal frame (low inundation depths), and (2) a landscape state with a lower resistance against flow (tidal flat) due to the absence of vegetation and a lower position in the tidal frame (greater inundation depths). It was found that during drainage and flooding of the vegetated tidal marsh, the flow was concentrated in and routed through the bare tidal channels, whereas on the unvegetated tidal flat more homogeneous sheet flow occurred. For the tidal marsh, sheet flow also occurred but only once the vegetation becomes overtopped. These differences in flow hydrodynamics result in different landform properties for the two landscape states. With regard to the platform, it was found that the tidal marsh has a clear levee-basin topography potentially influencing flow patterns, while this levee-basin topography is absent for the tidal flat.

In this study it was possible to substantiate previous claims on the effect of vegetation acting as a frictional constraint on flow routing. Additionally we could hint that vegetation not only directly influences flow patterns through increased friction, but also indirectly through its induced micro-topography of levees and basins. This was visible through the delayed platform flooding before vegetation submergence and the delayed platform drainage after vegetation emergence, ultimately adding important information precipitating a deeper understanding of bio-geomorphic systems.

Acknowledgements

We wish to thank Koen Ysebaert, Jean Waucomont, Marijke Ooms, Johnny Teuchies, Olivier Beauchard and Thorsten Balke for their kind assistance during field work. We thank Stichting Het Zeeuwse Landschap for giving permission for the field work; the Netherlands Institute of Ecology for assistance with the use of ADCPs; Nortek B.V. for use of an ADCP

724 as part of a Nortek Student Equipment Grant to the first author; Rijkswaterstaat (D.J. De
725 Jong) for use of aerial photos and LiDAR data. This study was partly funded by FWO-
726 Flanders (grant number 1503907N).
727
728
729

Figures

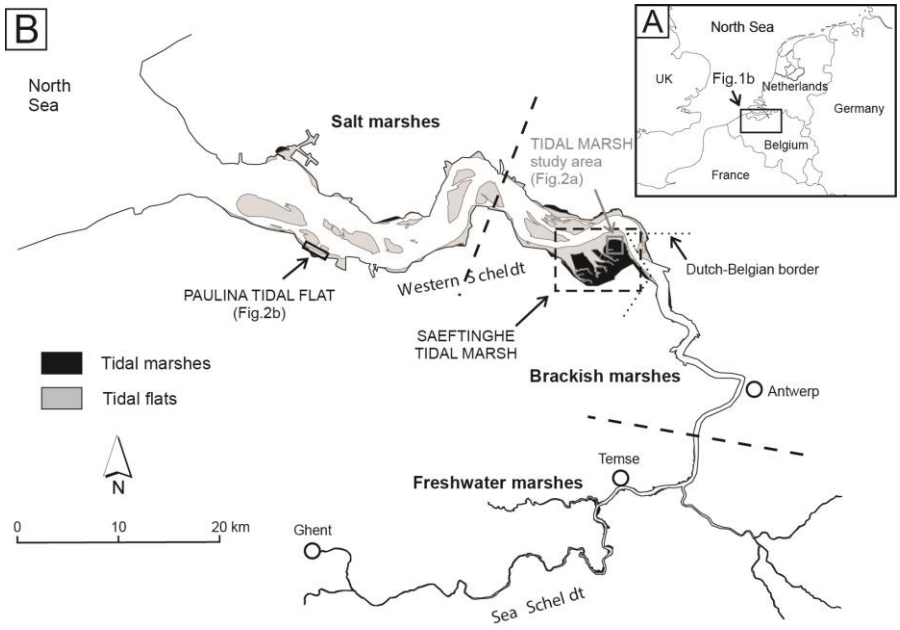

Fig. 1 The Scheldt estuary. (a) Location within Western Europe. (b) Location of the salt, brackish and freshwater tidal marshes (separated by dashes lines), location of the vegetated tidal marsh (Saeftinghe) and unvegetated tidal flat (Paulina) study area

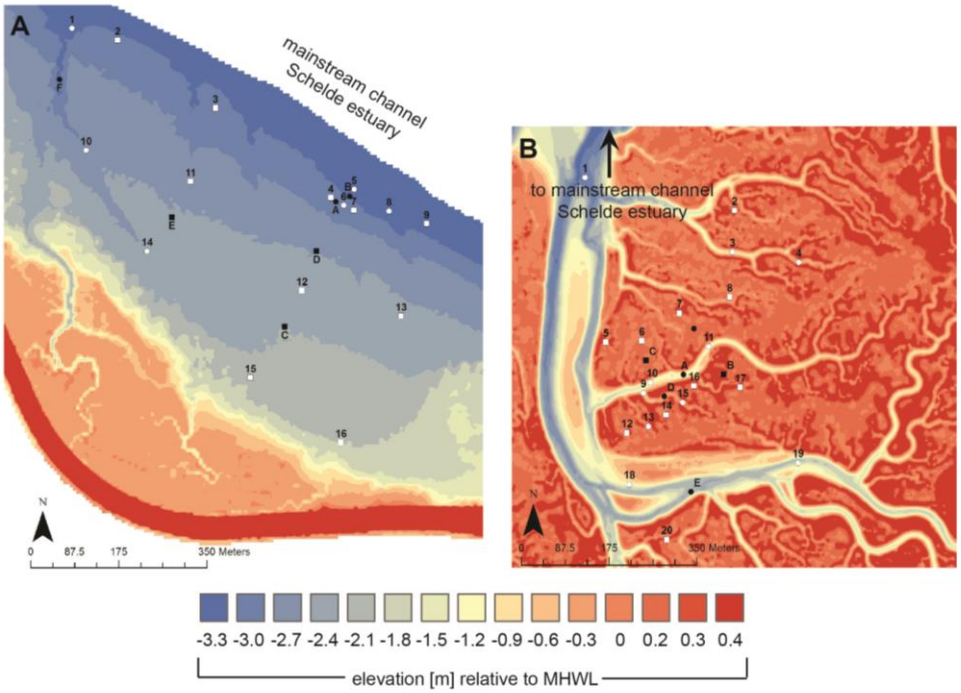

Fig. 2 Contour Map of the the unvegetated tidal flat (a) (Paulina, WGS84 coordinates: 51°21’10”N / 3°43’20”E) and vegetated tidal marsh (b) (Saeftinghe, WGS84 coordinates: 51°22’02”N / 4°11’10”E). White symbols are the locations where water levels were measured, with the circles the locations in the channels and the squares the locations on the platform. Black symbols are the locations of flow measurement, with the circles the locations in the channels and the squares the locations on the platform.

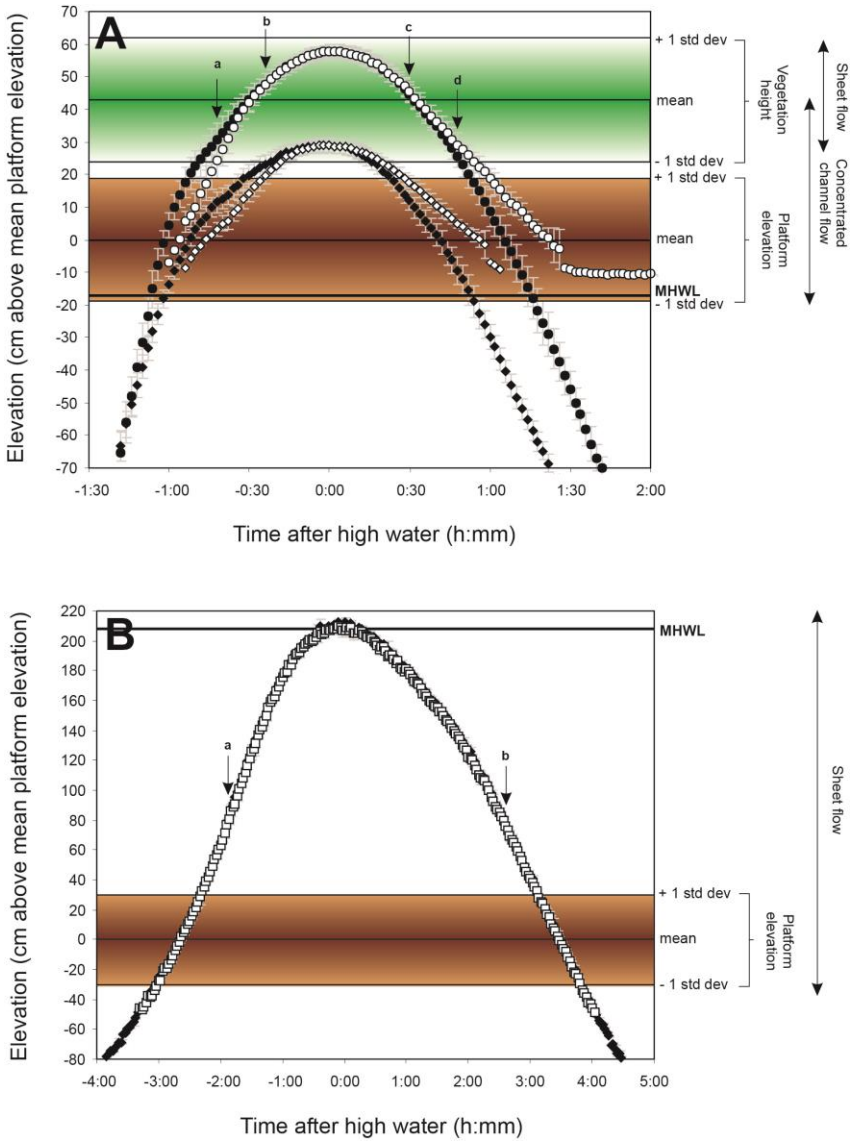

Fig. 3 (a) Comparison between the instantaneous mean water level (cm above mean platform elevation) in the marsh channels (black markers) and on the marsh platform (white markers) for a high inundation event which almost entirely overtops the vegetation cover (circles) and a medium high inundation event which does not submerge the vegetation cover (diamonds). (b) Comparison between the instantaneous mean water level (cm above mean platform elevation) in the tidal flat channels (black markers) and on the tidal flat platform (white markers) for one inundation event. Arrows indicate the time steps of the instantaneous water surfaces presented in Fig. 4 (arrows a-d) and 5 (arrows a-b).

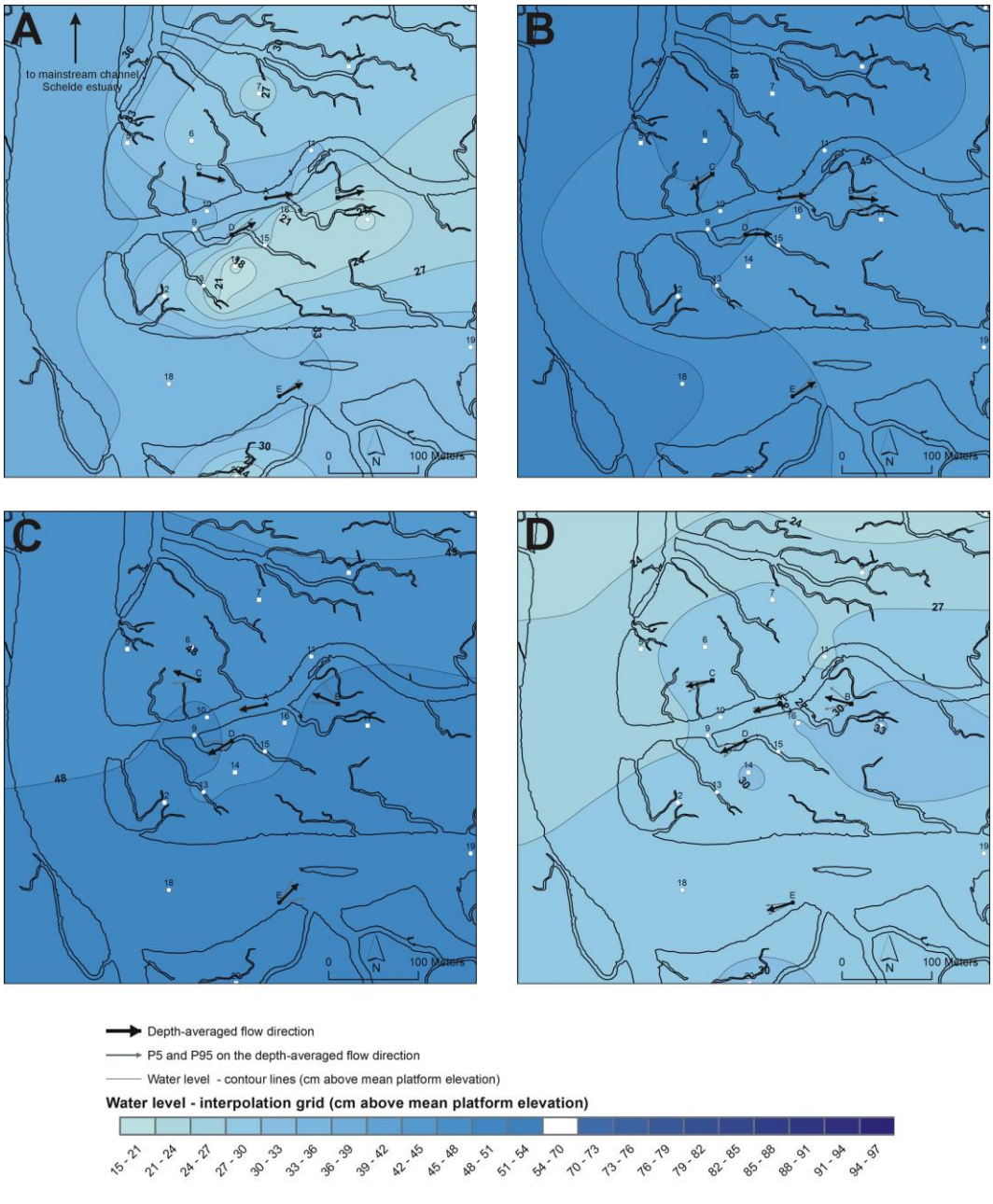

Fig. 4 Contour maps of instantaneous water surfaces (in cm above mean platform elevation) for the highest observed tide over the vegetated tidal marsh, for two time steps during the flood phase (a and b) and two time steps during the ebb phase (c and d). Time steps are indicated on Fig. 3a. Black arrows represent the depth-averaged flow directions, grey arrows the 5th and 95th percentile on the depth-averaged flow directions. The contour maps are only presented for the area with the highest density of water level stations (see Fig. 2a)

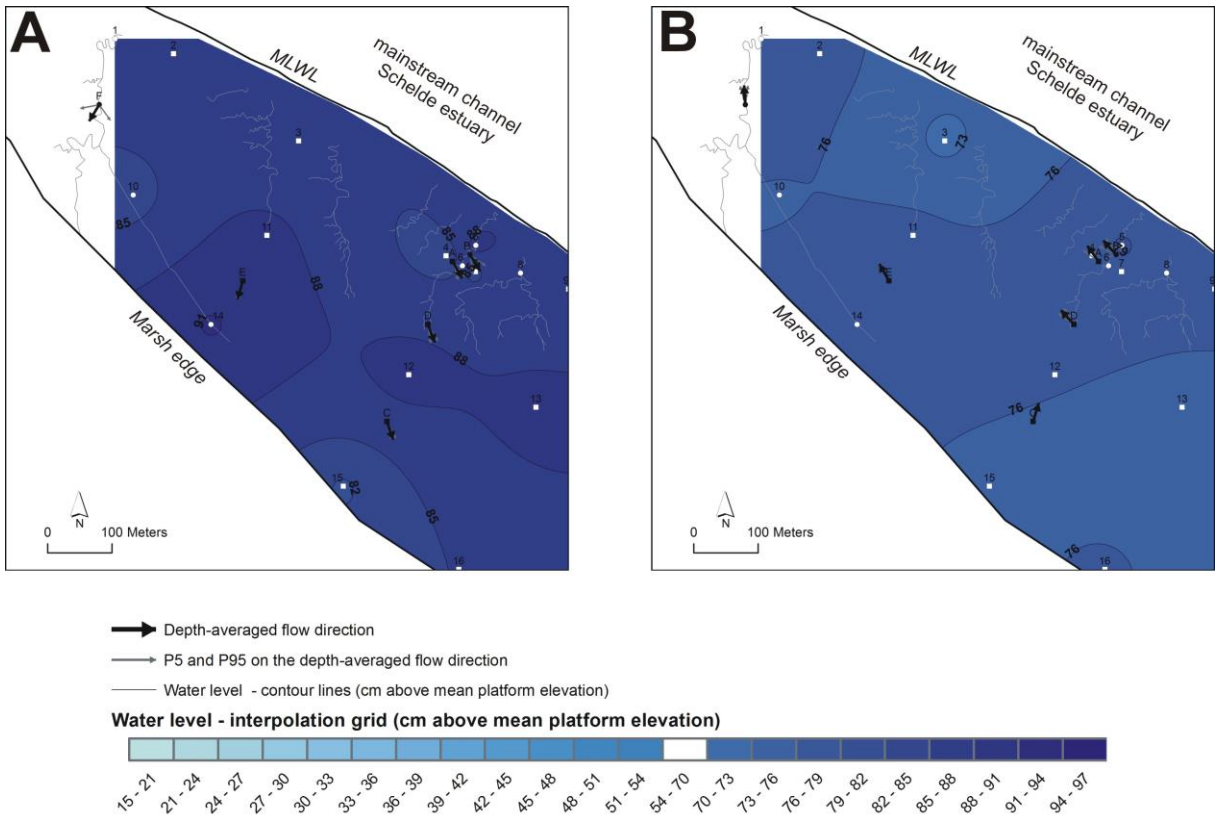

Fig. 5 Contour maps of instantaneous water surfaces (in cm above mean platform elevation) for the highest observed tide over the unvegetated tidal flat, for one time step during the flood phase (a) and one time step during the ebb phase (b). Time steps are indicated on Fig. 3b. Black arrows represent the depth-averaged flow directions, grey arrows the 5th and 95th percentile on the depth-averaged flow directions

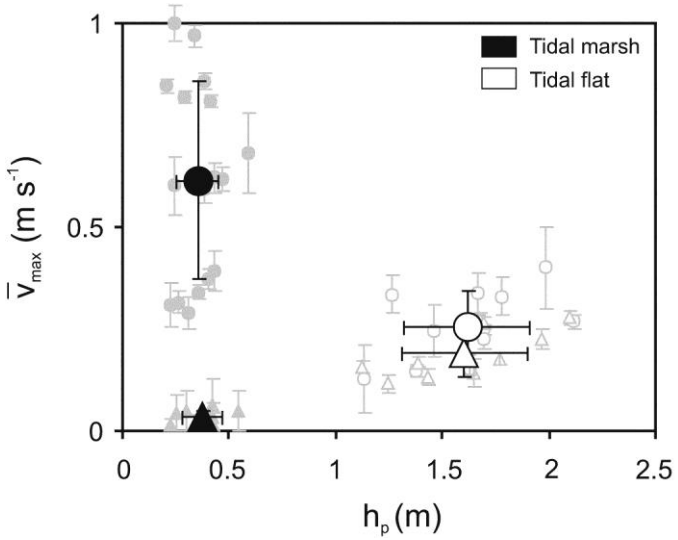

Fig. 6 (a) Maximum depth-averaged flow velocity of platform flow relative to tidal channel flow for all observed tides at our measurements location pairs at the marsh (AB and CD, see Fig. 2) and at the tidal flat (AB and DF, see Fig. 2). (b) Maximum inundation height over the platform (h_p) versus the maximum depth-averaged flow velocity ($\bar{v}_{max}$) for all observed tides (grey symbols). Measurements in the tidal marsh and tidal flat are represented by, respectively, the solid and empty symbols, and measurements in the channels and on the platform, respectively, by the circles and triangles. Mean values over all tides are represented by the large black symbols (solid = tidal marsh; empty = tidal flat).

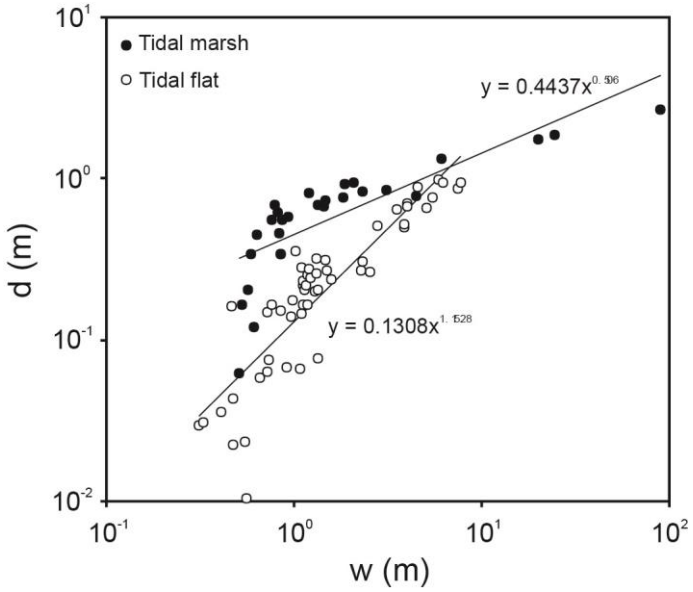

Fig. 7 Relationship between channel width (w) and channel depth (d) for a vegetated tidal marsh and an unvegetated tidal flat

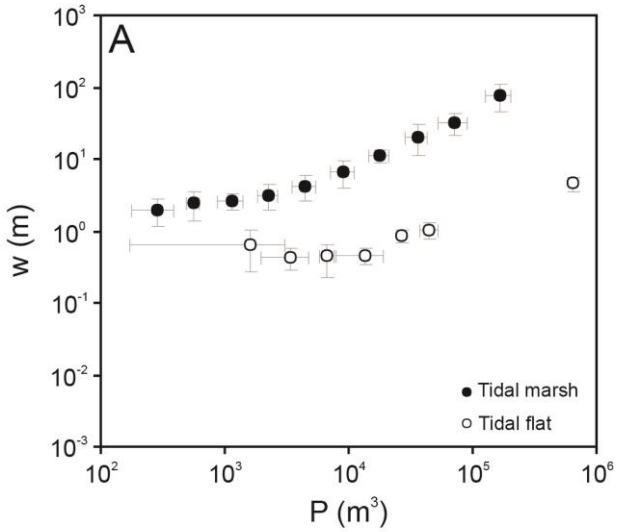
A
w (m)
P (m³)
Tidal marsh
Tidal flat

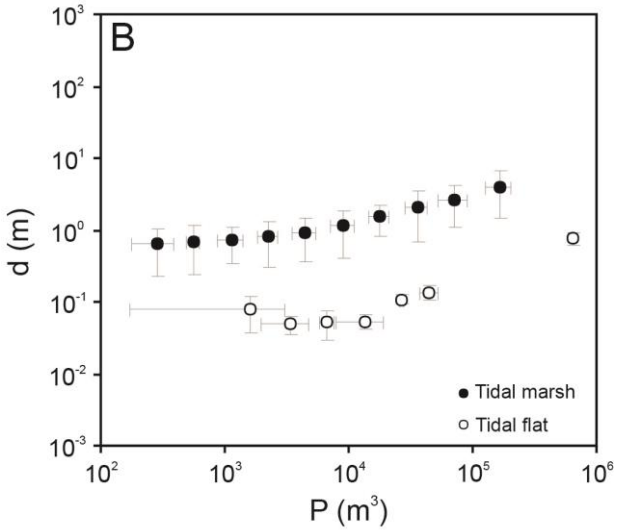
B
d (m)
P (m³)
Tidal marsh
Tidal flat

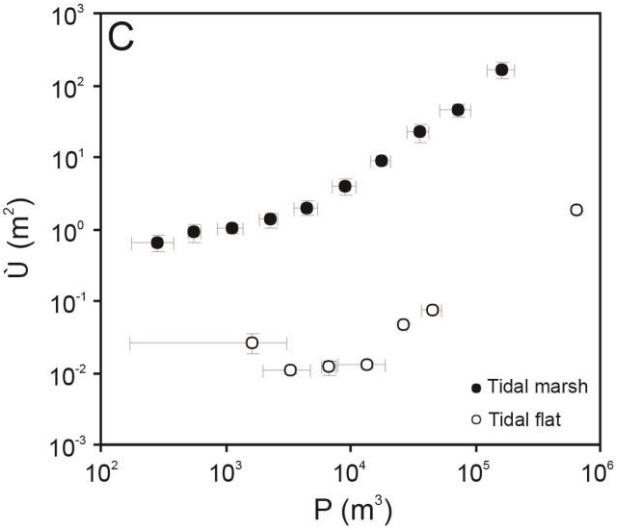
C
Ù (m²)
P (m³)
Tidal marsh
Tidal flat

912 Fig. 8 Tidal prism (P) versus the channel width (w), the channel depth (d) and the cross-
913 sectional area (Ω) (respectively panels a, b and c), for a vegetated tidal marsh and an
914 unvegetated tidal flat
915

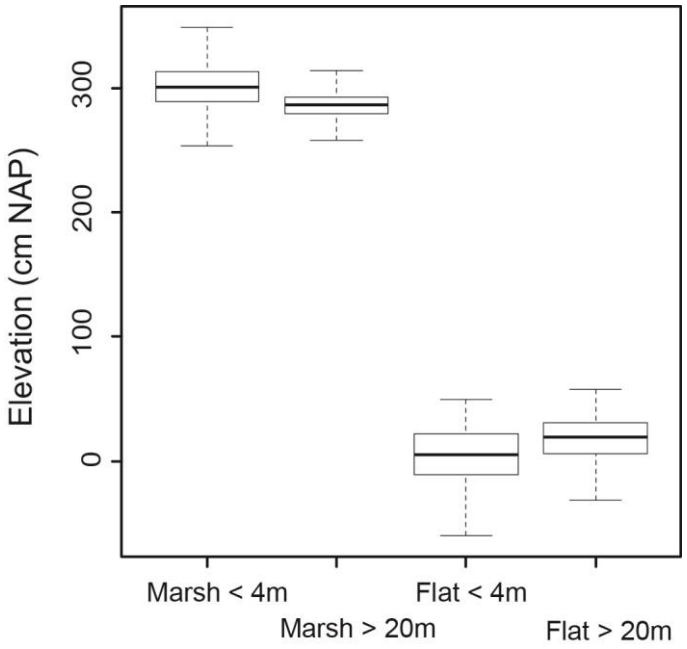

Fig. 9 Boxplots of the tidal marsh and tidal flat platform elevation, close to the channel edges (≤ 4 m) and further away from the channel edges (> 20 m).

References

Allen, J.R.L., 1990. Constraints on measurement of sea-level movements from salt-marsh accretion rates. Journal of the Geological Society of London 147, 5-7.

Allen, J.R.L., 2000. Morphodynamics of Holocene salt marshes: a review sketch from the Atlantic and Southern North Sea coasts of Europe. Quaternary Science Reviews, 19(12), 1155-1231.

Baas, A.C.W., Nield, J.M., 2007. Modelling vegetated dune landscapes, Geophysical Research Letters, pp. L06405.

Bayliss-Smith, T.P., Healey, R., Lailey, R., Spencer, T., Stoddart, D.R., 1979. Tidal flow in salt marsh creeks. Estuarine Coastal and Shelf Science 9, 235-255.

Blanton, J.O., Garrett, A.J., Bollinger, J.S., Hayes, D.W., Koffman, L.D., Amft, J., Moore, T., 2010. Transport and retention of a conservative tracer in an isolated creek-marsh system. Estuarine Coastal and Shelf Science 87, 333-345.

Bouma, T.J., Friedrichs, M., van Wesenbeeck, B.K., Temmerman, S., Graf, G., Herman, P.M.J., 2009. Density-dependent linkage of scale-dependent feedbacks: a flume study on the intertidal macrophyte Spartina anglica. Oikos 118, 260-268.

Bouma, T.J., Temmerman, S., van Duren, L.A., Martini, E., Vandenbruwaene, W., Callaghan, D.P., Balke, T., Biermans, G., Klaassen, P.C., van Steeg, P., 2013. Organism traits determine the strength of scale-dependent bio-geomorphic feedbacks: A flume study on three intertidal plant species. Geomorphology, 180, 57-65.

Braudrick, C.A., Dietrich, W.E., Leverich, G.T., Sklar, L.S., 2009. Experimental evidence for the conditions necessary to sustain meandering in coarse-bedded rivers. Proceedings of the National Academy of Sciences of the United States of America 106, 16936-16941.

Callaghan, D.P., Bouma, T.J., Klaassen, P., van der Wal, D., Stive, M.J.F., Herman, P.M.J., 2010. Hydrodynamic forcing on salt-marsh development: Distinguishing the relative importance of waves and tidal flows. Estuarine Coastal and Shelf Science 89, 73-88.

Christiansen, T., Wiberg, P.L., Milligan, T.G., 2000. Flow and sediment transport on a tidal salt marsh surface. Estuarine Coastal and Shelf Science 50, 315-331.

Claessens, J., Meyvis, L., 1994. Overzicht van de tijwaarnemingen in het Zeescheldebekken gedurende het decennium 1981-1990, Ministerie van de Vlaamse Gemeenschap AWZ Afdeling Maritieme Schelde, Antwerpen.

Collins, D.B.G., Bras, R.L., Tucker, G.E., 2004. Modeling the effects of vegetation-erosion coupling on landscape evolution, Journal of Geophysical Research, pp. F03004.

Corenblit, D., Gurnell, A.M., Steiger, J., Tabacchi, E., 2008. Reciprocal adjustments between landforms and living organisms: Extended geomorphic evolutionary insights. Catena 73, 261-273.

Craft, C., Clough, J., Ehman, J., Joye, S., Park, R., Pennings, S., Guo, H., Machmuller, M., 2008. Forecasting the effects of accelerated sea-level rise on tidal marsh ecosystem services. Frontiers in Ecology and the Environment, 7(2), 73-78.

Davidson-Arnott, R.G., van Proosdij, D., Ollerhead, J., Schostak, L., 2002. Hydrodynamics and sedimentation in salt marshes: examples from a macrotidal marsh, Bay of Fundy. Geomorphology, 48(1), 209-231.

D'Alpaos, A., Lanzoni, S., Mudd, S.M., Fagherazzi, S., 2006. Modeling the influence of hydroperiod and vegetation on the cross-sectional formation of tidal channels. Estuarine Coastal and Shelf Science 69, 311-324.

D'Alpaos, A., Lanzoni, S., Marani, M., Rinaldo, A., 2007. Landscape evolution in tidal embayments: modeling the interplay of erosion, sedimentation, and vegetation dynamics. Journal of Geophysical Research 112, 1-17.

D'Alpaos, A., Lanzoni, S., Marani, M., Rinaldo, A., 2010. On the tidal prism - channel area relations. Journal of Geophysical Research-Earth Surface 115, -.

Dietrich, W.E., Perron, J.T., 2006. The search for a topographic signature of life. Nature 439, 411-418.

Etheridge, J.R., Birgand, F., Burchell II, M.R., 2014. Quantifying nutrient and suspended solids fluxes in a constructed tidal marsh following rainfall: The value of capturing the rapid changes in flow and concentrations. Ecological Engineering.

Fagherazzi, S., Bortoluzzi, A., Dietrich, W.E., Adami, A., Lanzoni, S., Marani, M., Rinaldo, A., 1999. Tidel networks 1. Automatic network extraction and preliminary scaling features from digital terrain maps. Water Resources Research 35, 3891-3904.

Fagherazzi, S., Wiberg, P.L., Temmerman, S., Struyf, E., Zhao, Y., Raymond, P.A., 2013. Fluxes of water, sediments, and biogeochemical compounds in salt marshes. Ecological Processes, 2(1), 1-16.

French, J.R., Stoddart, D.R., 1992. Hydrodynamics of salt marsh creek systems: implications for marsh morphological development and material exchange. Earth Surface Processes and Landforms 17, 235-252.

Garofalo, D., 1980. The influence of wetland vegetation on tidal stream channel migration and morphology. Estuaries, 3(4), 258-270.

Hutchinson, M.F., 1989. A new procedure for gridding elevation and stream line data with automatic removal of spurious pits. Journal of Hydrology 106, 211-232.

Istanbulluoglu, E., Bras, R.L., 2005. Vegetation-modulated landscape evolution: effects of vegetation on landscape processes, drainage density, and topography, Journal of Geophysical Research, pp. F02012.

Jarrett, J.T., 1976. Tidal Prism-Inlet Area Relationship, CERC-WES General Investigation of Tidal Inlets, Dept. of the Army, U.S. Corps of Engineering.

Kirwan, M., Temmerman, S., 2009. Coastal marsh response to historical and future sea-level acceleration. Quaternary Science Reviews 28, 1801-1808.

Kirwan, M.L., Murray, A.B., 2007. A coupled geomorphic and ecological model of tidal marsh evolution. Proceedings of the National Academy of Sciences of the United States of America 104, 6118-6122.

Kirwan, M.L., Guntenspergen, G.R., D'Alpaos, A., Morris, J.T., Mudd, S.M., Temmerman, S., 2010. Limits on the adaptability of coastal marshes to rising sea level. Geophysical Research Letters 37, -.

Larsen, L.G., Harvey, J.W., 2011. Modeling of hydroecological feedbacks predicts distinct classes of landscape pattern, process, and restoration potential in shallow aquatic ecosystems. Geomorphology 126, 279-296.

Lawrence, D.S.L., Allen, J.R.L., Havelock, G.M., 2004. Salt marsh morphodynamics: An investigation of tidal flows and marsh channel equilibrium. Journal of Coastal Research 20, 301-316.

Leonard, L.A., Croft, A.L., 2006. The effect of standing biomass on flow velocity and turbulence in Spartina alterniflora canopies. Estuarine Coastal and Shelf Science 69 325-336.

Lightbody, A.F., Nepf, H.M., 2006. Prediction of velocity profiles and longitudinal dispersion in emergent salt marsh vegetation. Limnology and Oceanography 51, 218-228.

Marani, M., Lanzoni, S., Zandolin, D., Seminara, G., Rinaldo, A., 2002. Tidal meanders. Water Resources Research 38, Art. No. 1225.

Marani, M., Belluco, E., D'Alpaos, A., Defina, A., Lanzoni, S., Rinaldo, A., 2003. On the drainage density of tidal networks. Water Resources Research 29, Art. No. 1040.
Marani, M., D'Alpaos, A., Lanzoni, S., Carniello, L., Rinaldo, A., 2007. Biologically-controlled multiple equilibria of tidal landforms and the fate of the Venice lagoon, Geophysical Research Letters, pp. L11402.
Mariotti, G., Fagherazzi, S., 2010. A numerical model for the coupled long-term evolution of salt marshes and tidal flats. Journal of Geophysical Research-Earth Surface 115.
Meire, P., Ysebaert, T., Van Damme, S., Van den Bergh, E., Maris, T., Struyf, E., 2005. The Scheldt estuary: a description of a changing ecosystem. Hydrobiologia 540 1-11.
Mudd, S.M., Fagherazzi, S., Morris, J.T., Furbish, D.J., Fagherazzi, S., Marani, M., Blum, L.K., 2004. Flow, sedimentation, and biomass production on a vegetated salt marsh in South Carolina: toward a predictive model of marsh morphologic and ecologic evolution, The Ecogeomorphology of Tidal Marshes. American Geophysical Union Coastal and Estuarine Studies, Washington DC.
Mudd, S.M., D'Alpaos, A., Morris, J.T., 2010. How does vegetation affect sedimentation on tidal marshes? Investigating particle capture and hydrodynamic controls on biologically mediated sedimentation. Journal of Geophysical Research-Earth Surface 115.
Murray, A.B., Paola, C., 2003. Modelling the effect of vegetation on channel pattern in bedload rivers. Earth Surface Processes and Landforms 28, 131-143.
Murray, A.B., Knaapen, M.A.F., Tal, M., Kirwan, M.L., 2008. Biomorphodynamics: Physical-biological feedbacks that shape landscapes, Water Resources Research, pp. W11301.
Myrick, R.M., Leopold, L.B., 1963. Hydraulic geometry of a small tidal estuary. US Government Printing Office Washington, DC.
Nepf, H.M., 1999. Drag, turbulence, and diffusion in flow through emergent vegetation. Water Resources Research, 35(2), 479-489.
Neumeier, U., Amos, C.L., 2006. The influence of vegetation on turbulence and flow velocities in European salt-marshes. Sedimentology 53 259-277.
O'Brien, M.P., 1931. Estuary tidal prisms related to entrance areas. Civil Engineering, 1(8), 738-739.
O'Brien, M.P., 1969. Equilibrium flow areas of inlets on sandy coasts Journal of the Waterway and Harbour Divisions, ASCE 95, 43-52.
Pethick, J.S., 1980. Velocity surges and asymmetry in tidal channels. Estuarine Coastal and Shelf Science 11, 331-345.
Pethick, J.S., 1981. Long-term accretion rates on tidal salt marshes. Journal of Sedimentary Petrology 51, 571-577.
Reinhardt, L., Jerolmack, D., Cardinale, B.J., Vanacker, V., Wright, J., 2010. Dynamic interactions of life and its landscape: feedbacks at the interface of geomorphology and ecology. Earth Surface Processes and Landforms 35, 78-101.
Rinaldo, A., Fagherazzi, S., Lanzoni, S., Marani, M., Dietrich, E., 1999. Tidal networks 2. Watershed delineation and comparative network morphology. Water Resources Research 35, 3905-3917.
Rominger, J.T., Lightbody, A.F., Nepf, H.M., 2010. Effects of Added Vegetation on Sand Bar Stability and Stream Hydrodynamics. Journal of Hydraulic Engineering-Asce 136, 994-1002.
Schwarz, C., Ye, Q., Wal, D., Zhang, L., Bouma, T., Ysebaert, T., Herman, P., 2014. Impacts of salt marsh plants on tidal channel initiation and inheritance. Journal of Geophysical Research: Earth Surface, 119(2), 385-400.

Tal, M., Paola, C., 2007. Dynamic single-thread channels maintained by the interaction of flow and vegetation. Geology 35, 347-350.
Tal, M., Paola, C., 2010. Effects of vegetation on channel morphodynamics: results and insights from laboratory experiments. Earth Surface Processes and Landforms 35, 1014-1028.
Temmerman, S., Bouma, T.J., Govers, G., Lauwaet, D., 2005a. Flow paths of water and sediment in a tidal marsh: relations with marsh developmental stage and tidal inundation height. Estuaries 28, 338-352.
Temmerman, S., Bouma, T.J., Govers, G., Wang, Z.B., De Vries, M.B., Herman, P.M.J., 2005b. Impact of vegetation on flow routing and sedimentation patterns: Three-dimensional modeling for a tidal marsh, Journal of Geophysical Research, pp. F04019.
Temmerman, S., Bouma, T.J., Van de Koppel, J., Van der Wal, D., De Vries, M.B., Herman, P.M.J., 2007. Vegetation causes channel erosion in a tidal landscape. Geology 35, 631-634.
Temmerman, S., Moonen, P., Schoelynck, J., Govers, G., Bouma, T.J., 2012. Impact of vegetation die-off on spatial flow patterns over a tidal marsh. Geophysical Research Letters 39, 5.
Temmerman, S., Meire, P., Bouma, T.J., Herman, P.M., Ysebaert, T., De Vriend, H.J., 2013. Ecosystem-based coastal defence in the face of global change. Nature, 504(7478), 79-83.
Vandenbruwaene, W., Temmerman, S., Bouma, T.J., Klaassen, P.C., De Vries, M.B., Callaghan, D.P., Van Steeg, P., Dekker, F., Van Duren, L.A., Martini, E., 2011. Flow interaction with dynamic vegetation patches: Implications for biogeomorphic evolution of a tidal landscape. Journal of Geophysical Research-Earth Surface 116.
Vandenbruwaene, W., Meire, P., Temmerman, S., 2012. Formation and evolution of a tidal channel network within a constructed tidal marsh. Geomorphology 151, 114-125.
Vandenbruwaene, W., Meire, P., Temmerman, S., Bouma, T.J., 2013. Bio-geomorphic effects on tidal channel evolution: impact of vegetation establishment and tidal prism change. Earth Surface Processes and Landforms 38(2): 122-132.
Wamsley, T.V., Cialone, M.A., Smith, J.M., Atkinson, J.H., Rosati, J.D., 2010. The potential of wetlands in reducing storm surge. Ocean Engineering 37, 59-68.
Zong, L.J., Nepf, H., 2010. Flow and deposition in and around a finite patch of vegetation. Geomorphology 116, 363-372.
.